Modeling of novel resist technologies

Luke Long[1,3], Andrew Neureuther[2,3], and Patrick Naulleau[3]

[1]Department of Physics, University of California, Berkeley, CA, USA 94720
[2]Department of EECS, Univ. of California, Berkeley, CA, USA 94720
[3]Center for X-Ray Optics, Lawrence Berkeley National Laboratory, Berkeley, CA, USA 94720

February 2019

Abstract

In response to the difficulties posed by the resolution, line edge roughness, sensitivity (RLS) trade-off to traditional chemically amplified resist (CAR) systems used for extreme ultraviolet lithography, a number of novel resist technologies have been proposed. In this paper, the effect of quencher loading on three resist technologies is analyzed via an error propagation-based resist simulator. In order of increasing novelty as well as complexity, they are: conventional CAR with quencher, CAR with photodecomposable base, and PSCAR 2.0, a CAR system with photodecomposable base as well as an EUV-activated UV-sensitive resist component. Simulation finds the more complicated resist systems trade in an increase in resist stochastics for improved deprotection slopes, yielding a net benefit in terms of line width roughness.

1 Introduction

Chief among the remaining challenges for the insertion of extreme ultraviolet lithography (EUV) in high volume manufacturing are the problems posed by resist stochastics and the RLS tradeoff. Fundamentally, these challenges make it difficult to simultaneously achieve the resolution (R) required for continued device scaling, features smooth and predictable enough to meet device requirements (L), and sensitivity (S) required for the process to be economical. It has been shown that these challenges are fundamentally a result of the quantum nature of light and matter[1][2][3]. In order to smooth out the naturally grainy images produced by these quantized interactions, CAR utilizes incoming radiation to produce photoacid that, in effect, spatially averages the exposure energy by catalytically reacting with its host polymer environment. However, this averaging comes at a cost as the acid blur does not discriminate between dose variations due to photon and chemical shot noise and those due to the patterns produced by the mask. As a result, if the diffusion of each acid becomes too great, the resolution of the lithography process as a whole is reduced.

One strategy to limit acid diffusion is the addition of basic quencher molecules (referenced interchangeably as "base" and "quencher" in this paper) to neutralize the generated photo-acid. While this has proven an effective way to limit the acid blur, previous work has shown that it comes at a cost in terms of resist stochastics [3][4]. In order to mitigate the negative stochastic effects of quencher and to increase the photospeed of the resist, some resists have been engineered with photodecomposable base (PDB), a photoactive base that self-quenches when activated by EUV light. Previous modeling work suggests that in printing 25nm line/space patterns, this system has the potential to reduce the LER at a given dose relative to a conventional quencher [5]. In this paper, we reexamine the LWR/Dose trade-offs of conventional CAR (NPDB) and PDB in printing 16nm line/space patterns. We then extend the analysis to PSCAR 2.0[6], a relatively new member of the CAR lineage that utilizes the initial EUV patterning step to activate a photosensitizer which can in turn be used to produce more acid during an UV exposure step.

2 Model Description

The multivariate Poisson propagation model (MPPM) was used to analyze the effect of quencher loading on the LWR performance of the studied resists. Details of this model can be found elsewhere[2][3][7]; here we will summarize the main features and characteristics. The model assumes that the initial distribution of chemical components and photons is the main driver of resist stochastics. Furthermore, it treats the quanta as random variables, distributed in the resist according to Poisson statistics. Mean values are given by the nominal chemical loading and the aerial image intensity for the material components and photons, respectively. In addition, the film quantum yield of each photon[8] is also treated as a random variable. The combination of PAG, photon, and yield random variables combine to produce an initial acid image. In this way, acid stochastics are treated as a random variable derived from the combination of PAG, photon, and yield random variables. The acid image, along with a stochastic base image is fed into a deterministic reaction/diffusion simulation of the post-exposure bake, where the generated acids react with the host polymer in order to produce a deprotection image. In this way, the "error" of the initial component distributions is propagated through the bake process. The deprotection image can then be analyzed using a commercially available lithography analysis software[9] to obtain the resulting CD, LWR, PSD, etc. of the simulated patterns.

A key feature of this model is that it allows any subset of the random variables to be treated deterministically[2]. In this way, the impact of each individual random variable can be studied separate from the others. This analysis allows for the identification of the main stochastic culprits in terms of their contribution to LWR.

3 Modeling Approach

3.1 Input parameters

The input aerial image was the simulated output of a 16nm 1:1 line/space pattern from a 0.3 NA exposure tool. The approach of this study was to analyze the impact of quencher loading in the three systems under study by adjusting the dose as necessary to maintain a 16nm post-development CD. All other parameters were held constant as the base loading was changed, except the total quantum yield of PDB and PSCAR. The reasons for a quantum yield that is dependent on base concentration are discussed in Section 3.2. In this way, the effect of base loading was simulated using an approach comparable to one a resist chemist might employ to optimize base loading via experiment. Table 1 shows the input parameters to the model. f(Base) indicates the base loading dependence of the quantum efficiency in PDB resist.

Table 1: Input Parameters

Parameter	**Value**
PAG	$0.2/nm^3$
Base	Variable
$blur_{Acid}$	$12nm$
$blur_{Base}$	$6nm$
$blur_{electron}$	$2nm$
k_{ab}	$10nm^3/s$
$k_{deprotection}$	$3nm^3/s$
QE_{NPDB}	2.08
QE_{PDB}	f(Base)
absorptivity	$4.3/\mu m$

3.2 Modeling of PDB

A prototypical PDB consists of a photoactive group attached to a basic quenching ion such as hydroxide[10]. Upon photodecomposition, the base group associates with a proton produced via the decomposition of the photoactive

group. The base is thus used to quench its own photogenerated acid, lowering the quencher concentration in the exposed regions of the resist. In this model, it is assumed that the proximity of the base group and the acid produced by photodecomposition leads to an instantaneous quenching reaction. Furthermore, it is assumed that this reaction is irreversible. Thus, any additional acid produced by the decomposition of base contributes only to reducing the local quencher concentration, not to deprotection of the polymer.

3.3 PSCAR 2.0 Modeling

While a more detailed picture of PSCAR 2.0 can be found in [6], a summary is provided here. PSCAR is an extension of the CAR lineage, differing from its more conventional counterparts by the addition of a spatially-controlled UV sensitizer step. A schematic of the process produced by the model can be found in Figure 1, which compares qualitatively to those presented in [6]. In PSCAR 2.0, the initial EUV exposure step is used to produce acids as well as decompose base. This initial chemical distribution then activates a photosensitizer from its precursor molecule during a room temperature reaction step. In the process, acid and base from the initial exposure react, increasing the chemical gradient. Upon exposure to UV light, the sensitizers can further activate PAG and decompose base. Finally, the post exposure bake induces the reaction diffusion process as in the conventional resists.

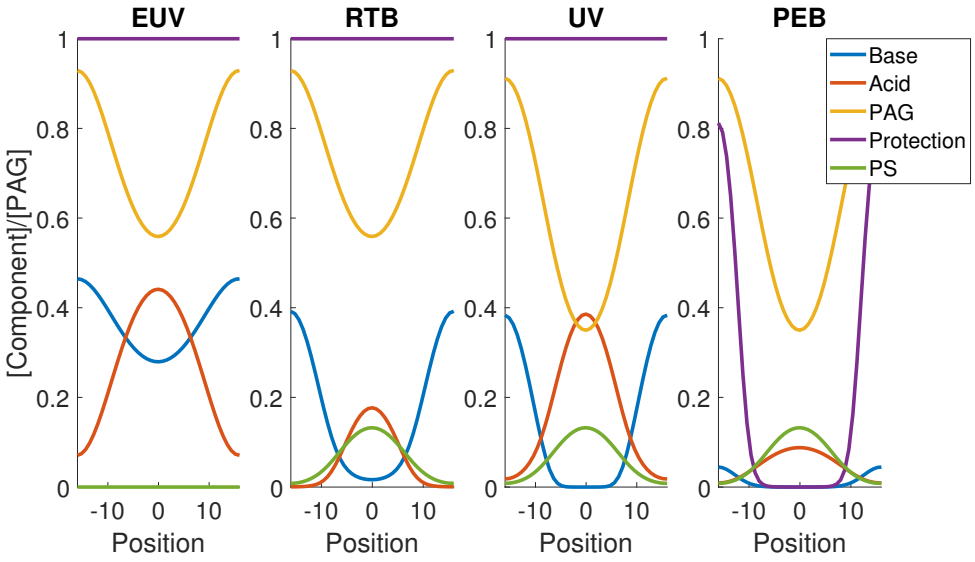

Figure 1: PSCAR 2.0 Process.

3.4 Quantum Efficiency Modeling

As the number of electrons per EUV photon is finite, introduction of PDB will induce a competition for photo-electrons between PAG and PDB. A model is thus required to partition the efficiency of each photon between the PAG and PDB. Consistent with previous modeling on PDB with the MPPM [5], the total quantum efficiency was modeled according to a saturation equation as illustrated experimentally in reference [8]. The maximum achievable QE was set to 4.5 based on the experimental data, and the exponential coefficient set such that the PAG loading alone gives a QE of 2.08. Then a new total QE was calculated according to the total amount of photo-active compound ($PAC = PAG + PDB$), which was then split between the PAG and PDB according to their fraction of total PAC. The QE equaitons are shown in Equation 1. As seen in Figure 2, the effect adding PDB thus increases the total QE, but decreases the efficiency of each photon with respect to PAG activation. We further note that this simple model could be modified if, for example, the cross section of the electron-PAG interaction differed substantially from that of the electron-PDB interaction.

$$QE_{tot}(PAC) = QE_{sat} exp[-\alpha PAC] \tag{1a}$$

$$QE_{PAG}(PAC) = \frac{PAG}{PAC} QE_{tot}(PAG) \tag{1b}$$

$$QE_{Base}(PAC) = \frac{Base}{PAC} QE_{tot}(PAG) \tag{1c}$$

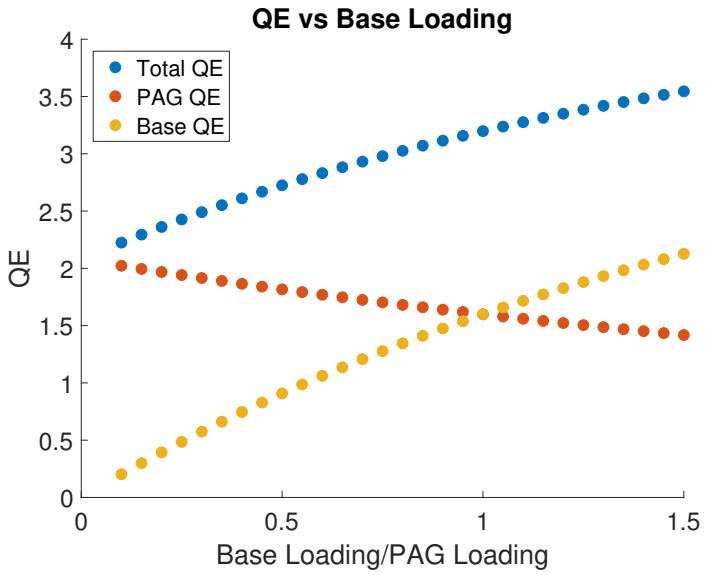

Figure 2: Quantum efficiencies as a function of base loading for NPDB resist. As base loading increases, the overall QE increases, but acid generation efficiency decreases due increased photoelectron competition.

3.5 Modeling of UV Sensitization in PSCAR

In order to model additional acid generation in PSCAR via UV exposure, a random variable for the quantum efficiency of the photosensitizers was used. As the UV dose used during this step is on the order of J/cm^2[6], the UV photons are not expected to be significant contributors to the overall resist stochastics. However, there is still certain to be some fluctuation in the number of activation events stemming from each photosensitizer (PS) due to randomness in the sensitization process. The quantum yield variable is intended to account for this randomness.

Of additional concern in the PSCAR 2.0 system is that the photosensitizers are capable of decomposing base as well as activating PAG. A simple model predicts that the relative probabilities of PAG activation and base decomposition are given by the relative concentrations of each component. As in the discussion above, the result would be a decrease in the acid yield per sensitizer as the concentration of PDB is increased. However, because UV photons are essentially free in comparison to their EUV counterparts, it was assumed that the UV dose can be increased in the presence of PDB in order to keep the PAG yield constant. These additional photons apply themselves to the decomposition of PDB. In sum, the net efficiency of the sensitizers was modeled as a linearly increasing function of PDB concentration, owing itself to an underlying increase in UV dose.

3.6 Simplified Models

While the MPPM provides numerical simulation results, the trends can be challenging to interpret. In this section, several simplified models are put forth which are useful in understanding the simulation results.

3.6.1 Noise/Slope

It has been established that LER originates from a combination of deprotection noise and deprotection slope[1][11]. In essence, this captures the fact that LER is a function of how much the deprotection at the nominal line edge is deviating from the developable threshold, and when it does, how far that deviation shifts the realized line edge. This idea is represented mathematically in Equation 2. As validation that the MPPM adheres to this relationship, Figure 3 compares the LER as measured in SuMMIT and that computed via the noise/slope model. The good agreement suggests that fluctuations in the line edge position can be analyzed in terms of two terms: the numerator of Equation 2, which encompasses the various stochastic components as they propagate to the deprotection image, and the denominator, which accounts for the deterministic conversion of aerial image to deprotection profile.

$$LER = \frac{3\ \sigma_D}{\frac{dD}{dx}} \tag{2}$$

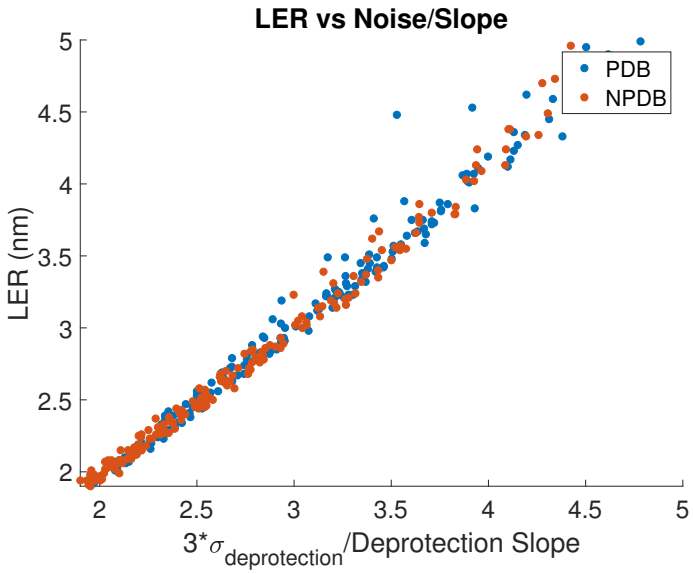

Figure 3: Measured LER vs Noise/Slope model.

3.6.2 Relative Noise

A previously published model[3] of relative noise is useful in understanding stochastics in the deprotection image. In summary, this simplified model treats the net acid (A) as the sum over the number of absorbed photons (P) of the yield (Y) of each photon, minus the amount of base quencher (Q). Each of P,Y, and Q are independent random variables. Using the tools of probability, the expectation value and variance of net acid can be calculated. As deprotection is ultimately a relative quantity, and as it stems directly from the acid-deprotection reaction, this model provides a simplified picture of the origins of deprotection noise. This model for net acid, as well as its expectation value and variance are shown in Equation 3.

$$A = \sum_{i}^{P} Y_i - Q \tag{3a}$$

$$E[A] = E[P]E[Y] - E[Q] \tag{3b}$$

$$Var[A] = E[P]Var[Y] + Var[P]E[Y]^2 + Var[Q] \tag{3c}$$

This model can be extended for use in the case of a photodecomposable base. Here, an extra term needs to be added to account for the additional yield from each photon dedicated to decomposing base. The modified simple noise model is shown in Equation 4. These equations will be examined in further detail in the results section.

$$A = \sum_{i}^{P} YA_i - Q + \sum_{i}^{P} YQ_i \tag{4a}$$

$$E[A] = E[P]E[YA] - E[Q] + E[P]E[YQ] \tag{4b}$$

$$Var[A] = E[P](Var[YA] + Var[YQ]) + Var[P](E[YA] + E[YQ])^2 + Var[Q] \tag{4c}$$

4 Results

4.1 LWR

Figure 4 contains the MPPM LWR and dose vs base loading results for the three resist platforms studied. We will begin the discussion with the conventional base resist data (blue). Consistent with previous modeling [3][4], as well as experiment [12], an increase in base loading initially leads to a reduction in LWR, bottoming out at a value of about 3.6 nm at 55% base loading for the parameter set used in this study. After this point, increasing the base loading leads to an increase in LWR. In addition, Figure 4 shows that, as expected, the dose to size increases rapidly as a function of base loading. In comparison, for both PDB and PSCAR 2.0, LWR strictly decreases as a function of the base loadings simulated. More importantly, the LWR for PDB and PSCAR is less than that of NPDB at the same dose, with the PSCAR and PDB LWR curves nearly overlapping. For the more complicated resist types, the dose to size is a linear function of base loading. Additionally, as would be expected based on an increase in total quantum efficiency, the required dose at a given base loading is less when the base is photodecomposable. Because quencher is destroyed during exposure, base loading can be higher than PAG loading in PDB and PSCAR. The moderate increase in dose at each base loading for PSCAR in comparison to PDB is due to some of the initial acid produced during the EUV step being spent during the room temperature reaction process and not recovered by sensitization. In the following sections, these results are analyzed, with an emphasis on whether the noise, slope, or both is responsible for the improvement in LWR at a given dose for PDB and PSCAR 2.0.

4.2 Noise

Deprotection noise at line edge as a function of dose can be found in Figure 5. Comparison with Figure 4 shows that improvements in deprotection noise are not responsible for the lower LWR at a given dose in PDB and PSCAR 2.0, as PDB is noisier than NPDB, and PSCAR is the noisiest of the three. Additionally, the LWR trend in NPDB does not match the noise trend. Nevertheless, Equations 3 and 4 can be used to compare the noise values for each of the resist types. The comparison suggests that the variance of the net acid increases at a given dose when the base becomes photodecomposable due to the increase in the total quantum efficiency of the material. In essence, because each photon plays a bigger role in the net acid produced, the overall importance of the photon shot noise is enhanced. In PSCAR, because the initial acid is responsible for activating the sensitizers, which in turn produce more acid, there is even more emphasis on these initial photons.

In Figure 6, the deprotection noise at line edge is plotted as function of dose when each of the various noise terms is treated separately from the others. For NPDB, it is seen that at all but the lowest doses, the base is the dominant contributor to deprotection noise. As suggested by Poisson statistics, the relative importance of the photon shot noise decreases as the dose increases, as does the quantum yield. The noise due to base, however, remains more or less constant as the base loading (and thus dose) increases. This imposes a material limit on the noise performance of the resist given a set of blurs and reaction rates that cannot be improved upon even in the limit of zero photon shot noise. This material limit is discussed in [3]. In PDB, the absolute noise from base alone is similar to that in NPDB. However, as heuristically argued above, the photon noise is greater. As the quencher loading is increased, the increased workload of each photon effectively amplifies the photon shot

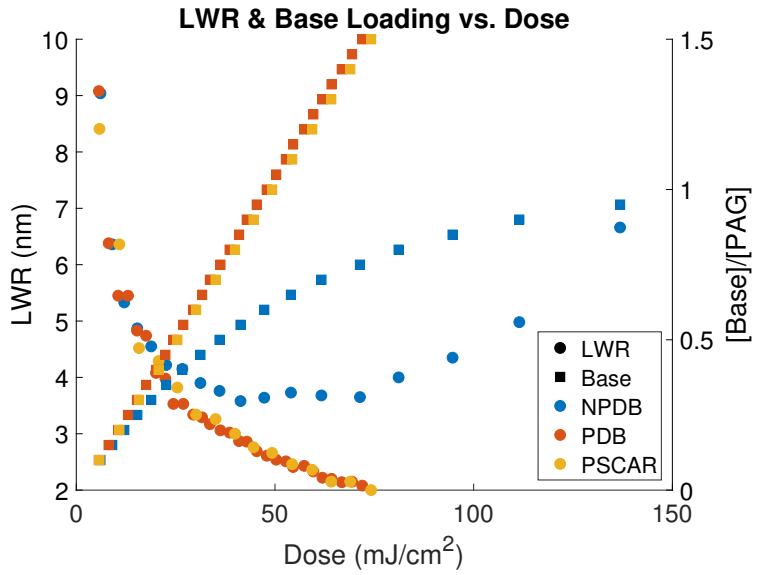

Figure 4: LWR vs Dose for all three resist platforms. The different colors refer to the photoresist type, while circles correspond to LWR (left) and squares refer to base loading (right).

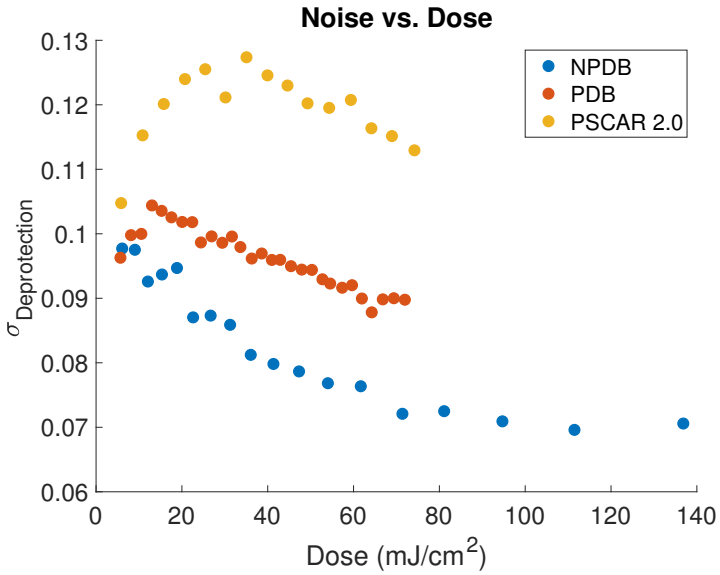

Figure 5: Total Noise vs. Dose

noise relative to NPDB. In other words, while the actual distribution of photons at a given dose is the same for the three resist platforms, the effect of that noise on the deprotection image is magnified. PSCAR 2.0, also containing PDB, shows similar noise trends, with additional emphasis on the initial photons as previously argued. The base contribution also increases as it helps to shape the sensitizer image and thus the acid image responsible for deprotection during PEB.

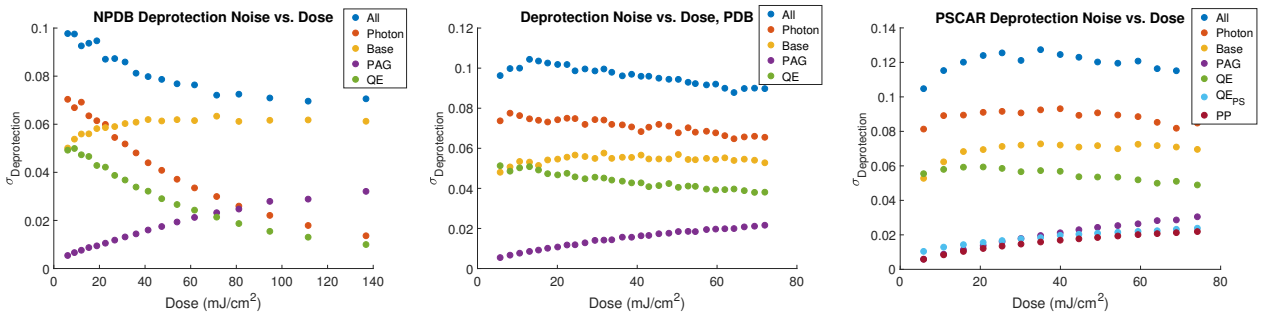

(a) NPDB Contributions (b) PDB Contributions (c) PSCAR 2.0 Contributions

Figure 6: Breakout of different noise contributions

4.3 Slope

The noise/slope model suggests that if PDB and PSCAR produce noisier deprotection images, then they must also produce images with better slopes in order to to achieve improved LWR. As seen by comparing Figures 4 and 7, the general shape of the LWR vs dose curve matches that of the slope vs dose curve. This highlights the importance of the deprotection slope in determining the final LWR of the resist as reported in [12] and [5]. It is thus worth trying to understand the origin of the slope trends.

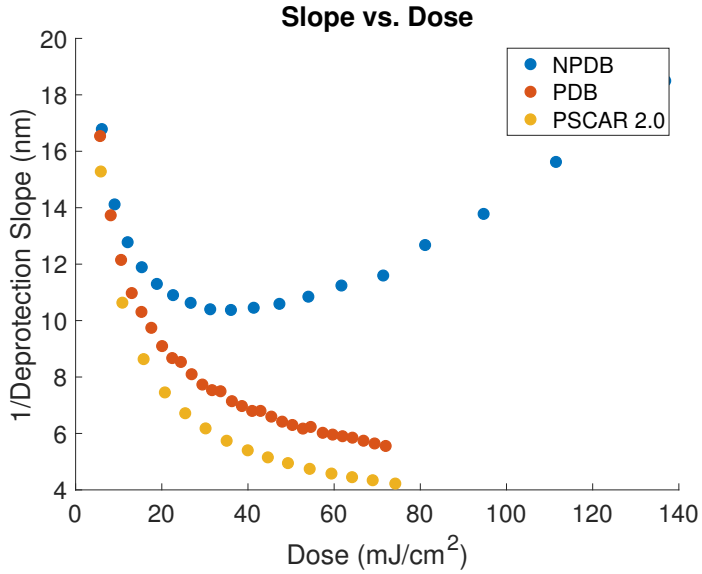

Figure 7: PSCAR 2.0 Slope vs Dose.

The beginning of the post exposure bake process is when the chemical gradients and concentrations are their highest. Thus, the most rapid reaction and diffusion happens during this period. A logical place to look for the root of the deprotection slope trends is thus the initial chemical concentrations before PEB. Figure 8 shows the initial acid and base profiles for three different base loadings in NPDB. Two things stand out from these profiles. The first is that, as the base loading increases, so does the absolute acid slope and amount of acid at the line edge, as expected. The second is that, at 80% base loading, the top of the acid peak is starting to become flatter than in the lower base loading profiles. This is due to the limited amount of PAG in the resist. As the resist becomes more and more saturated, extra dose pushes the saturated part of the acid profile out away from the center of the line toward the line edge, reducing the slope. This turn around in acid slope is evident in Figure

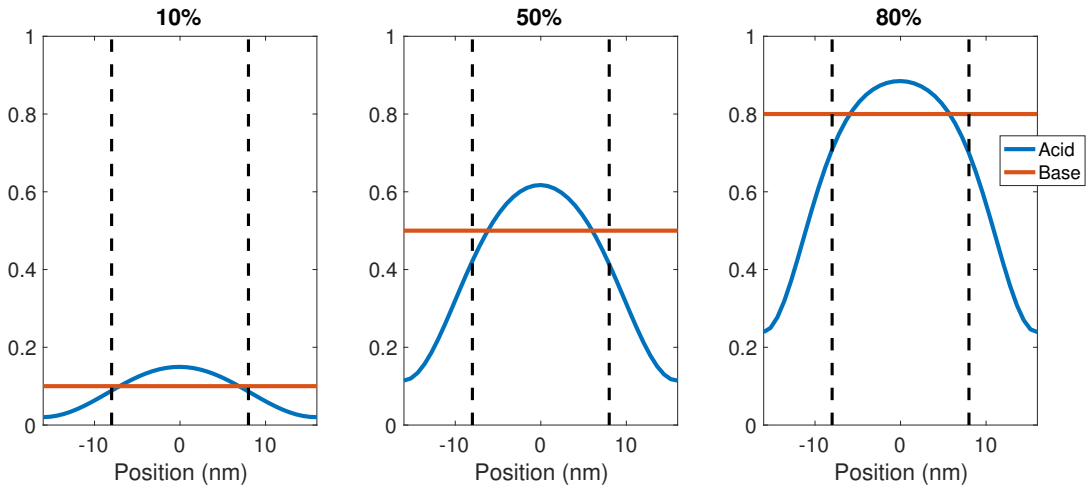

Figure 8: NPDB Acid Profiles. Concentrations normalized by PAG loading.

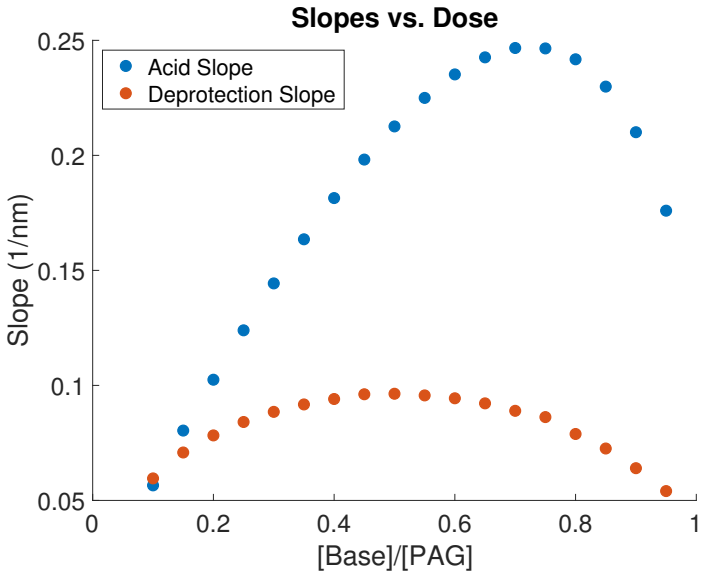

Figure 9: NPDB Acid and Deprotection Slopes.

9, though it happens at a higher base loading than the degradation of the deproteciton slope. This discrepancy can be ascribed to the cost of having extra acid at the line edge. Using the deprotection reaction rate equation, we can produce an equation for how the deprotection slope is changing in time:

$$\frac{\partial}{\partial x}[\frac{\partial \rho_D}{\partial t}] = \frac{\partial}{\partial x}[k_D \rho_{acid}(1-\rho_D)] \tag{5a}$$

$$\frac{\partial}{\partial t}[\frac{\partial \rho_D}{\partial x}] = k_D(\frac{\partial \rho_{acid}}{\partial x}(1-\rho_D) - \rho_{acid}\frac{\partial \rho_D}{\partial x}],. \tag{5b}$$

The first term on the right hand side of Equation 5b shows that the deprotection slope benefits from a large acid slope early in the reaction diffusion process. The second term, however, indicates that extra acid at the line edge degrades the slope as the deprotection gradient is built. Intuitively, this is due to saturation of deprotection: the deprotection rate in the highly exposed region of the resist slows as the number of protecting groups is reduced. If the amount of acid at the line edge is high, the result is that the deprotection in the ideally

unexposed region of the resist will begin to catch up to that in the highly exposed region. This in turn reduces the deprotection slope at the line edge. In the NPDB resist, the rate of acid slope increase is reduced as the PAG saturates, and the negative impact of extra acid at the line edge takes over, ultimately reducing the deprotection slope.

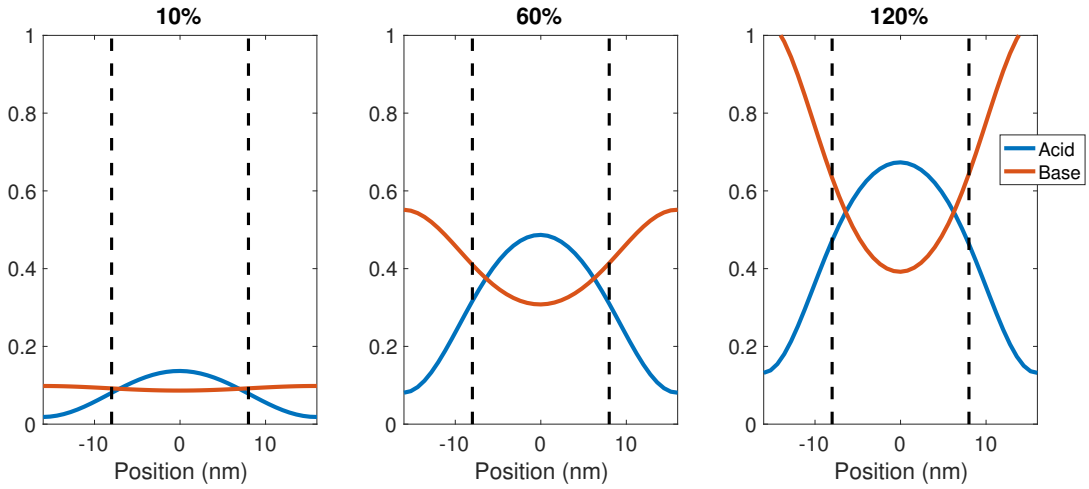

Figure 10: PDB Acid Profiles.

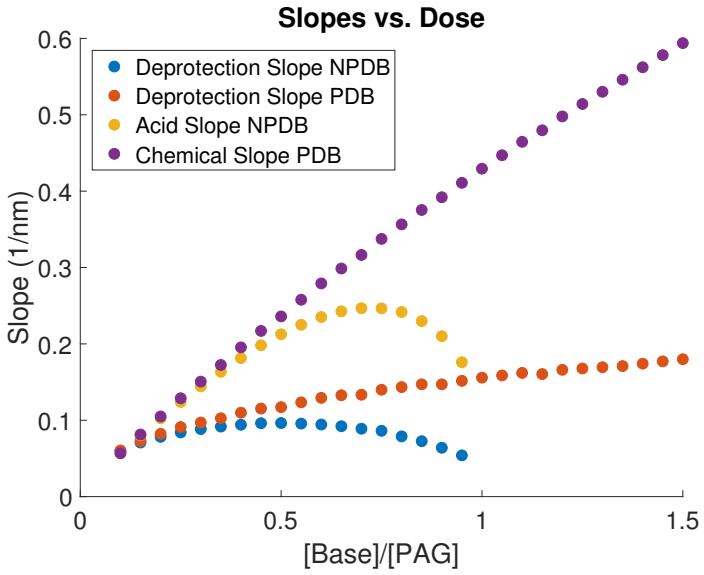

Figure 11: PDB Slope vs Dose.

In contrast, the slope for PDB and PSCAR improves as more base is added to the resist. Figure 10 shows the acid profile at three different base loadings of PDB. These profiles suggest two advantages for PDB over NPDB. The first is that, because the dose at a particular base loading is less in PDB than NPDB, the PAG stays far from saturation. The second is that both the base and acid profiles are sloped. If we assume that the net acid is simply acid minus base, this represents an increase in chemical slope as indicated in Figure 11. These improvements in the initial chemical image propagate through the bake to yield an improvement in deprotection slope. Finally, as compared to PDB, PSCAR 2.0 shows the best deprotection slopes of the three. In essence, this is due to the annihilation reaction that takes place at room temperature coupled with the ability to generate

more acid and decompose more base during the UV sensitization step. This combination of events produces a ravine in which the acid can diffuse and deprotect the polymer during PEB as illustrated in the third panel of Figure 1. This improvement in slope is dramatic enough to almost exactly cancel the impact of additional deprotection noise as compared to the PDB resist.

4.4 RLS Tradeoff

What do these results mean for the RLS tradeoff? While the sensitivity and LWR are straightforward to characterize, resist resolution is a somewhat more subjective metric of resist performance. Typical metrics such as correlation length do not capture the anisotropy of the deprotection process introduced by having both acid and quencher gradients. However, the deprotection slope captures the distance over which the resist is switched from developable to undevelopable and vice versa. The shorter this distance, the greater the number of lines and spaces can be packed per unit length. Thus, 1/slope can be used as a metric for the resolution of the resist. With this definition, Z factors defined by $Resolution^3 * LWR^2 * Sensitivity$ were calculated and plotted as a function of base loading in Figure 12. While PSCAR 2.0 shows no improvement over PDB in terms of LWR at a given dose, the improvement in deprotection slope suggests that the resolution of PSCAR 2.0 may exceed that of more conventional resist systems. Moreover, the RLS trade-off suggests that this "extra" resolution may be traded in to yield better sensitivity or LWR. However, this is dependent on how the chemical blurs used in this simulation compare to the optimal blur for each resist formulation[13].

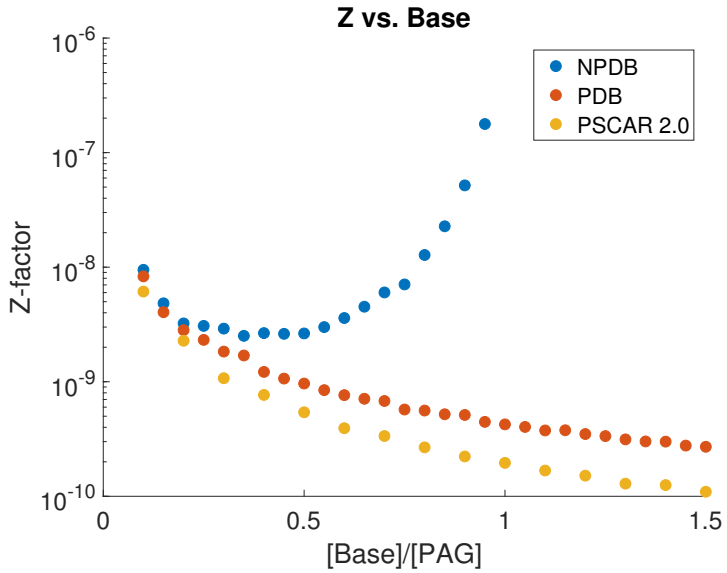

Figure 12: Z factor $(R^3 * (LWR)^2 * S)$.

5 Conclusion

Using the MPPM, we have analyzed the LWR/sensitivity trade-off for three resist systems as a function of base loading. The trends were analyzed in terms of the effect of base on the deprotection noise and slope, having shown that the quotient of these parameters yields the simulated LER. For PDB systems it can be shown that the system suffers from increased noise due to additional emphasis being placed on the initial photon distribution. However, an improvement in deprotection slope leads to an overall improvement in LWR for PDB as compared to conventional base. PSCAR 2.0 continues this trend, placing even more emphasis on the initial photons but further improving the slope. Our simulations indicate that PSCAR 2.0 shows similar LWR performance at a given dose to PDB, with both representing $\approx 20\%$ improvement in LWR at $40mJ/cm^2$. That being said, with

deprotection slope as the metric for resolution, our work suggests PSCAR 2.0 to be the best performing of the three resists studied in terms the RLS trade-off, with best-case Z factors improved by a factor of three relative to PDB. Ultimately, this work demonstrates the importance of the non-stochastic deprotection slope in mitigating the effect of chemical and photon shot noise, and suggests deprotection slope optimization as a strategy to beat the RLS trade-off.

6 Acknowledgements

This research is sponsored by C-DEN (Center for design-enable nanofabrication). Member companies ARM, ASML, Cadence, Carl Zeiss Group, Intel, KLA-Tencor, Mentor Graphics, and Qualcomm. This work was performed in part at Lawrence Berkeley National Laboratory which is operated under the auspices of the Director, Office of Science, of the U.S. Department of Energy under Contract No. DE-AC02-05CH11231. In addition, we would like to thank Seiji Nagahara of TEL for a number of valuable and engaging discussions.

References

[1] G. M. Gallatin, "Resist blur and line edge roughness," *Proceedings of SPIE* **5754**(May 2004), pp. 38–52, 2005.

[2] P. Naulleau, S. Bhattarai, A. Neureuther, W. Chao, and C. Anderson, "Studying Resist Stochastics with the Multivariate Poisson Propagation Model," *Journal of Photopolymer Science and Technology* **27**(6), pp. 747–750, 2015.

[3] P. Naulleau and G. Gallatin, "Relative importance of various stochastic terms and EUV patterning," *Journal of Micro/Nanolithography, MEMS, and MOEMS* **17**(04), p. 1, 2018.

[4] S. G. Hansen, "Photoresist and stochastic modeling," *Journal of Micro/Nanolithography, MEMS, and MOEMS* **17**(01), p. 1, 2018.

[5] S. Bhattarai, A. R. Neureuther, and P. P. Naulleau, "Simulation analysis of LER and dose tradeoffs for EUV resists with photo-decomposable quenchers," *Proceedings of SPIE* **8679**(April 2013), p. 867925, 2013.

[6] S. Nagahara, M. Carcasi, G. Shiraishi, H. Nakagawa, S. Dei, T. Shiozawa, K. Nafus, D. De Simone, G. Vandenberghe, H.-J. Stock, B. Küchler, M. Hori, T. Naruoka, T. Nagai, Y. Minekawa, T. Iseki, Y. Kondo, K. Yoshihara, Y. Kamei, M. Tomono, R. Shimada, S. Biesemans, H. Nakashima, P. Foubert, E. Buitrago, M. Vockenhuber, Y. Ekinci, A. Oshima, and S. Tagawa, "Photosensitized Chemically Amplified Resist (PSCAR) 2.0 for high-throughput and high-resolution EUV lithography: dual photosensitization of acid generation and quencher decomposition by flood exposure," *Proceedings of SPIE* **10146**(March 2017), p. 101460G, 2017.

[7] P. Naulleau, C. Anderson, W. Chao, S. Bhattarai, and A. Neureuther, "Stochastics and EUV Patterning in the 1x-nm Regime," *Journal of Photopolymer Science and Technology* **29**(6), pp. 797–802, 2016.

[8] R. Brainard, C. Higgins, E. Hassanein, R. Matyi, and A. Wüest, "Film Quantum Yields of Ultrahigh PAG EUV Photoresists," *Journal of Photopolymer Science and Technology* **21**(3), pp. 457–464, 2008.

[9] "SuMMIT LER Analysis, www.lithometrix.com."

[10] S. Funato, Y. Kinoshita, T. Kudo, S. Masuda, H. Okazaki, M. Padmanaban, N. Suehiro, and G. Pawlowski, "Photodecomposable a Novel Chemically Concept To Amplified Bases : Stabilize," *Journal Of Photopolymer Science And Technology* **8**(4), 1995.

[11] J. J. Biafore and M. D. Smith, "Application of stochastic modeling to resist optimization problems," *Advances in Resist Materials and Processing Technology XXIX* **8325**(March 2012), p. 83250H, 2012.

[12] T. B. Michaelson, A. R. Pawloski, A. Acheta, Y. Nishimura, and C. G. Willson, "The Effects of Chemical Gradients and Photoresist Composition on Lithographically Generated Line Edge Roughness," *Proceedings of SPIE* **5753**(May 2005), pp. 368–379, 2005.

[13] D. Van Steenwinckel, J. H. Lammers, T. Koehler, R. L. Brainard, and P. Trefonas, "Resist effects at small pitches," *Journal of Vacuum Science & Technology B: Microelectronics and Nanometer Structures* **24**(1), p. 316, 2006.